Experimental Research of Aerodynamic Noise Induced by Condenser of Drying Machine

Nikola Holeček†

Gorenje, P.O. Box 107, SI - 3503 Velenje, Slovenia

Brane Širok and Marko Hočevar

University of Ljubljana, Faculty of Mechanical Engineering, Aškerčeva cesta 6, SI - 1000 Ljubljana, Slovenia

Rudolf Podgornik

University of Ljubljana, Faculty of Mathematics and Physics, Jadranska 19, SI - 1000 Ljubljana, Slovenia

(Received 20 August 2004; accepted 27 October 2004)

In this paper analyse the noise of aerodynamic sources induced by a drying machine condenser. Two condenser versions of identical external geometry that differ in the form of the flow channel in the direction of the secondary flow, were studied. We analysed the integral and local aerodynamic and acoustic characteristics of both condenser types. The measured far-field sound frequency spectra show essential differences between the two cases, discernible in the form and location of specific peaks superimposed on a generic power-law frequency spectrum. Recent theoretical advances in the Lighthill acoustic analogy were used to identify the generic part of the spectrum due to isotropic turbulence. The specific peaks in the spectrum are apparently due to different structural characteristics of the two studied versions of the condenser types. The measured characteristics of the power spectra were used to propose optimisation strategies in the design of the acoustic properties of the drying machine condensers.

† Member of the International Institute of Acoustics and Vibration (IIAV)

1. INTRODUCTION

Energy consumption and noise emission are the most important functional characteristics of household clothes drying machines on the basis of which customers make their purchase decisions.[1] The condenser, whose energy characteristics make a particularly important imprint in the overall product evaluation, is one of the most important components of clothes drying machine. During the drying process, the primary airflow passes through the clothes drum and condenser, while the secondary airflow is used in cooling down the condenser and for driving the condensation process. In the design of clothes drying machines, the most important concerns are the energy efficient design of primary and secondary flow channels, are the proper selection of fans and condenser types. In assessing these production parameters, the sound power level and power frequency spectra are of primary importance. Thus, we set out to establish an approximate measure of the acceptance based on these measurable acoustic quantities that can be used in the evaluation and design of various condenser types.

In this work, we present a method to measure the sound power level and power frequency spectra of the noise of aerodynamic sources induced by the drying machine condenser. Our aim is to provide the condenser manufacturers with reliable parameters concerning the acoustic properties of condensers. Results of these measurements provide an insight into the strategy for the reduction of energy consumption of the drying machine.

The difference between various types of condensers can exceed 5 dB in A-weighted sound power level, when installed in the appliance, resulting in typical deviations in drying machine classifications that need to be considered in further development and optimisation. The noise level produced depends on the geometry of the channels and the aerodynamic characteristics of the airflow in the condenser flow channels. The most pronounced noise source of the condenser is the airflow at the outlet side of the secondary circuit, which is discharged directly into the environment. Another source of the difference between condensers can be determined by measuring their far-field sound power frequency spectrum that also shows pronounced variation with respect to the condenser type. We will show that for the two types of condensers investigated, their specificity can be ascertained by the presence and form of peaks in the sound power frequency spectrum.

In accordance with the Lighthill acoustic analogy,[2] the far-field sound intensity and sound spectrum are determined by different velocity correlators in the turbulent part of the airflow at the outlet side of the secondary circuit. Lighthill's acoustic analogy is based on a certain reformulation of the standard Navier-Stokes equations for the fluid flow that leads to an inhomogeneous wave equation for the fluctuating fluid density with quadrupole acoustic sources.[3] The complete flow problem in the far field approximation is thus substituted by a solution of an inhomogeneous wave equation with localised quadrupolar sources in the ambient flow at rest. These sources are described by the Lighthill's instantaneous applied acoustic strength tensor, T_{ij}. The central step in Lighthill's theory is the assumption that the applied acoustic strength tensor is spatially localised, thus, the far-field solution of the inhomogeneous wave equation is essentially reduced to the

evaluation of the fourth order two-point space-retarded time covariance of $\partial^2 T_{ij}/\partial t^2$ in a localised stationary volume. The sound power radiated to the far field is found by integration of this space-retarded time covariance over the localised acoustic source volume.

It is often convenient to approximate certain types of turbulent flow as if they were isotropic, since isotropic turbulence has no preferred direction and requires a minimum number of quantities to describe its characteristics.[4] The estimation of sound radiation from isotropic turbulence is an important step in the application of Lighthill's theory. For the total sound power $\bar{p}$ in the far field, Proudman found[5]

$$\bar{p} = \alpha\rho\frac{u^5}{c^5}\varepsilon\,, \tag{1}$$

where $u^2 = 2K/3$, K is the turbulent kinetic energy, c is the speed of sound, u is the flow velocity, ρ is the density in the far field, ε is the dissipation rate of the isotropic turbulence, and the presumably universal proportionality constant α, the Proudman constant, can be expressed in terms of the trace of the spatial velocity correlator of the turbulence.

The most essential and critical step in the evaluation of the sound power in the far-field is thus to find a proper form for the velocity correlators. This can be done only by invoking additional approximations and/or assumptions on the nature of the turbulent motion. Rubinstein and Zhou recently considered two hypotheses[6,7] on the nature of the turbulence that allowed them to derive two different limiting forms of the noise frequency spectra. We used them to fit and assess the non-specific component of the measured sound spectra. The two limiting forms of the sound spectrum were obtained theoretically: one leading to the form $\omega^{-4/3}$ and based on the dominance of sweeping by the largest energetic scales and the other one leading to the form $\omega^{-7/2}$ and based on the dominance of local straining.[8] These analytical estimates of the sound power spectra in the far-field approximation are the only ones that can be used in comparing our experimental data to theoretical predictions.

DNS computation, unfortunately, requires prohibitively high resolution in both space and time in order to compute fourth order time derivatives of the Lighthill stress tensor that would give an independent estimate of the acoustic spectral density of the noise.[9,10]

Using these recent results on the far-field frequency spectra, we were able to decompose the measured noise from a condenser into two components: 1) a non-specific one, stemming from the Lighthill mechanism and well described by the Rubinstein-Zhou result, and 2) a specific one, where one or more spectral peaks are superimposed onto a non-specific background, with the peaks' position and shape varying with the condenser type. It is this specific part of the frequency spectrum, embodied in the position and form of the peaks, that provides a quantitative measure of acoustic acceptance that can be used in the evaluation and design of various condenser types.

The plan of the paper is as follows: we first present measurement protocols and fundamental results on the sound intensity and frequency power spectra studied in the far-field case. Two type A condensers and one type B condenser were analysed. The channels of both type A condensers are made of fins transformed from sheet metal straps, whereas type B is provided with channels based on extruded composed profiles (Fig. 1). Both type A condensers have the same geometry, but they differ in the characteristics of their fins and their attachment to the structure of the condenser.

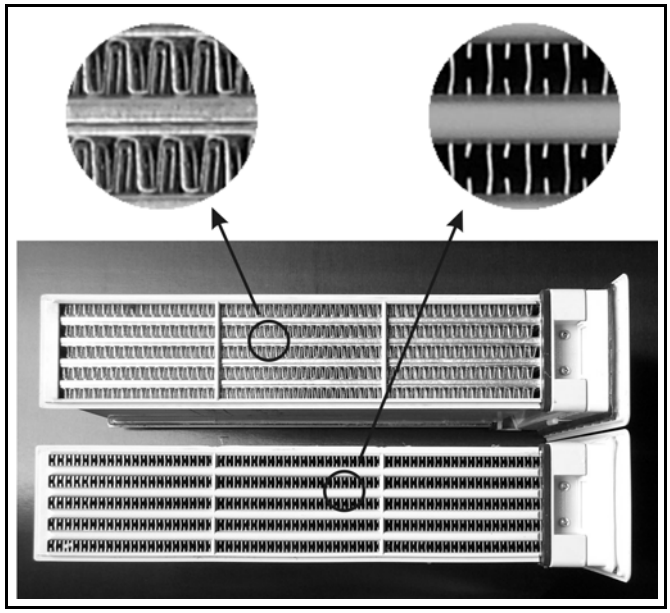

Figure 1. Type A condenser (top) and type B condenser (below) of domestic clothes dryer. The figure shows secondary flow channels.

2. METHODS

In order to analyse the characteristics of various condensers, we first constructed a measuring station. The measuring station allows for the assessment of aerodynamic and acoustical parameters of clothes drying machine condensers in both the primary and secondary flow. The measurements were performed at the outlet side of the secondary air circuit.

The measuring station (Fig. 2) is composed of four main units: a fan as the flow generator, a flow measuring unit, an attenuating and damping unit, and a measuring unit.

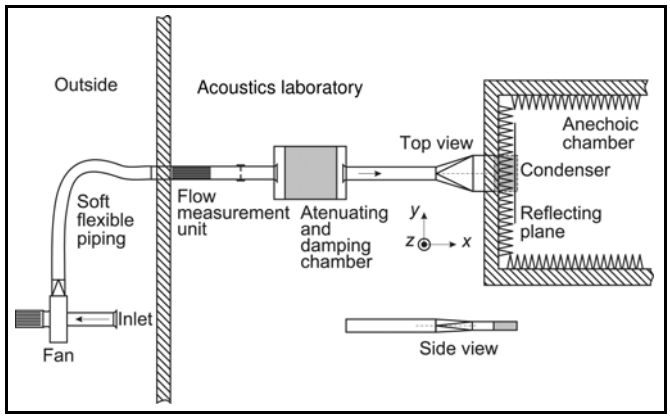

Figure 2. Schematics of experimental set-up. The fan was located outside the building and connected with the interior with the soft flexible piping. The flow measurement unit and attenuating chamber were located inside the acoustic laboratory, while the condenser was located in the anechoic chamber.

The fan is of a radial type and is fitted with a frequency inverter allowing regulation of the condenser operational point according to the selected volume flow. The fan was located outside the building and connected to the flow meas-

urement unit with soft flexible piping to eliminate the background noise and vibration of the fan. Other parts of the measuring unit were located inside the acoustics laboratory. The flow measuring unit contains an orifice plate, fitted into the flow system in accordance with the DIN 1952 standard.[11] The length of the straight part of the pipe in front of the orifice plate is 10*d*, and behind the orifice plate, 3*d*. The pipe diameter is $d = 150$ mm. A four-arm flow guide with a length of 2*d* behind the fan was used to eliminate vortices of the fan.

The third unit of the measuring station is an attenuating and damping chamber with a length of 1000 mm and a diameter of 600 mm. The flow slows down in the attenuating chamber. The attenuating chamber contains an 800 mm-thick glass wool layer to ensure reduction of noise generated by the fan.

The measuring unit is composed of a 10*d* long pipe, a transition element, and the element containing the built-in condenser. The transition element allows the transition from the round cross-section to the square cross-section and is executed with small angles to prevent flow separation. The measuring unit is coated with felt, preventing sound transmission from the measuring unit structure into the environment. The use of felt was adequate since the noise and vibration of the fan were completely suppressed with the soft flexible piping and within the attenuating and damping chamber. The felt was used only to reduce the structural noise generated by the turbulent properties of the flow inside the condenser. The measurement unit was placed in the anechoic chamber. For an accurate selection of the condenser working point, a fully gas-impermeable system was provided on the part from the orifice plate to the condenser.

3. EXPERIMENT

3.1. Measurement of Acoustical Characteristics

Measurements of the condensers' acoustical characteristics were performed in an anechoic room with a free space volume of 220 m³ ($7.8 \times 6.7 \times 4.2$ m). Its walls and ceiling are coated with a sound absorption cover in the form of polyurethane foam wedges. The wedges are 80 cm long. There is also a 5 cm layer of air between the wedges and walls. Measurements according to the ISO 3745[12] standard have been carried out for the anechoic chamber. They have shown that the lower limit frequency is 100 Hz, the A-weighted sound pressure level in the most unfavourable circumstances is 13 dB and the discrepancy from the legality "1/*R*" in the frequency range from 100 Hz to 10 kHz is admissible according to the standard.[13]

To carry out source sound power measurements according to the absolute method, a measuring system was used consisting of 10 FalconTM Range 1/2", type 4189 (B&K) microphones and 10 DeltaTron-Type 2671 microphone preamplifiers, connected via three BNC 2149 connection modules and linked to DSA interfaces NI 4552 dynamic signal analysers. The temperature, humidity, and ambient pressure sensors were connected to a TC 2190 module, together with a NI 4351 interface by a coaxial cable.

The location of the condenser in the acoustical chamber was 1.5 m from the entrance shaft, 3.35 m from both side walls, and 2.1 m above the ground. Sound pressure measurements were carried out at 10 positions on the surface of the hemisphere with a 1 m radius as a function of flow through the condenser (Fig. 3). The locations of the microphones for sound pressure measurements are presented in Table 1. An outlet funnel was fitted to the condenser outlet part and adjusted above the reflecting surface in the anechoic chamber.

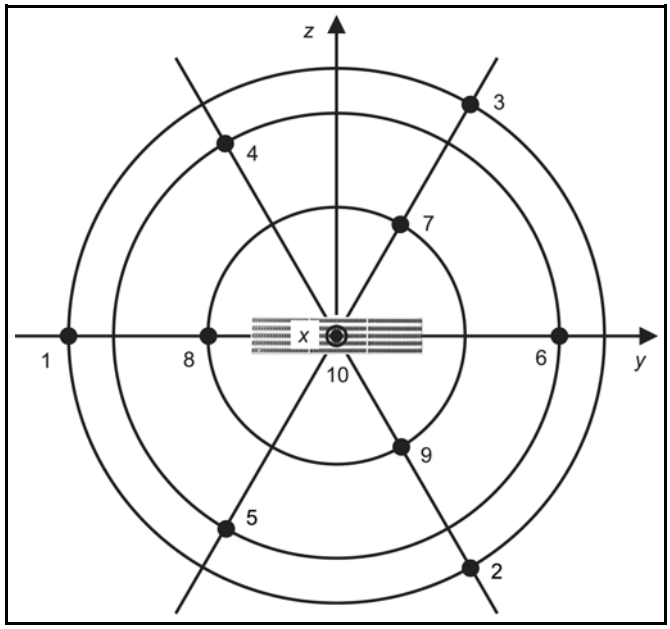

Figure 3. Microphone positions over a condenser at reflecting plane.

Table 1. Locations of microphones.

Mic.	*x* (m)	*y* (m)	*z* (m)
1	0.15	-0.99	0
2	0.15	0.5	-0.86
3	0.15	0.5	0.86
4	0.45	-0.45	0.77
5	0.45	-0.45	-0.77
6	0.45	0.89	0
7	0.75	0.33	0.57
8	0.75	-0.66	0
9	0.75	-0.33	-0.57
10	1	0	0

The sound pressure level frequency characteristics (1/3 octave) were measured at each measurement point. The sound pressure levels were corrected according to the background sound pressure levels using the equation

$$L_p = 10 \log(10^{0.1L_C} - 10^{0.1L_B}), \tag{2}$$

where L_p is the corrected value, L_C is the measured value, and L_B is the background noise level. The sound power level was calculated on the basis of the average sound pressure level on the measuring surface:

$$L_W = \overline{L_p} + 10 \log\left(\frac{S}{S_0}\right) + C;$$

$$C = -10 \log\left(\sqrt{\frac{293}{273+t}\frac{p}{1000}}\right), \tag{3}$$

where $\overline{L_p}$ is the calculated average sound pressure level, *r* is the hemisphere radius in m, $S = 2\pi r^2$ is the hemisphere surface in m², surface $S_0 = 1$ m², *t* is the operating ambient tem-

perature in °C, p is the ambient air pressure in mbar, and C is the correction factor in dB, taking account of the barometric pressure p in mbar and the temperature t in °C in the chamber.

Sound intensity measurements of condenser acoustical characteristics were performed with a two-channel analyser with a sound intensity probe in 21 measurement points, based on the method described by Crocker.[14] The location of the measurement points is shown in Fig. 4. The positioning of the sound intensity probe was performed by a computer controlled traversing system.

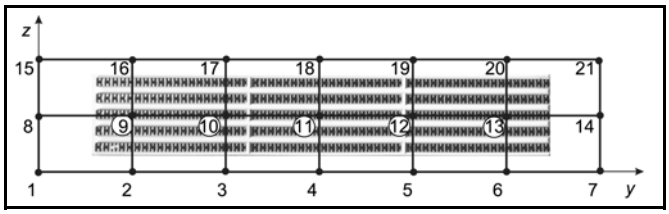

Figure 4. Measurement points for sound intensity measurements.

All measurement equipment was calibrated using a suitable piston phone and sound intensity calibrator with a valid calibration certificate from the competent authority.

3.2 Measurements of Aerodynamic Properties of the Flow

Beside measurements of the condensers, acoustical properties, measurements of the aerodynamic properties of the turbulent flow at the outlet side of the secondary circuit of the condenser were performed. Velocity field measurements were performed, with the aid of the traversing method, with a single-component hot-wire probe Dantec type 55P11 and an anemometer Dantec MiniCTA, which was connected to the data acquisition board in a personal computer that captured the data with a sampling rate of 50000 Hz. Total acquisition time was 4 s. The velocity was filtered using a low pass filter with a cut-off frequency of 10 kHz. The estimated uncertainty in the velocity measurements was ±3% of the average value. Velocity measurements were performed in the middle of the condenser's outlet plane at a distance of 3 mm from the condenser. Sound power spectra were calculated according to the Eq. (4).[4]

$$u(f) = \int_{-\infty}^{+\infty} u(t) e^{-i2\pi ft} dt \,. \qquad (4)$$

A hanning window was used to avoid aliasing problems.

4. RESULTS

The background noise at the measuring station was tested without the condenser. During all selected volume flows, the difference in A-weighted sound power level was more than 15 dB.

Figure 5 shows the total sound power level of the flow through the condenser for three condenser types, A1, A2, and B. We notice substantial differences in noise levels between individual condensers. Condenser A1 achieves the total sound power of 2.4 μW (63.9 dB) at the flow of 157 m^3/h. At the same flow rate, however, the sound power of condenser B is only 6.3 nW (38 dB).

The experimental sound power spectra of both types of condensers contain a non-specific spectral background on which one or more tones are superimposed. The intensity and to some extent the position of the peaks depend on the flow rate through the condensers.

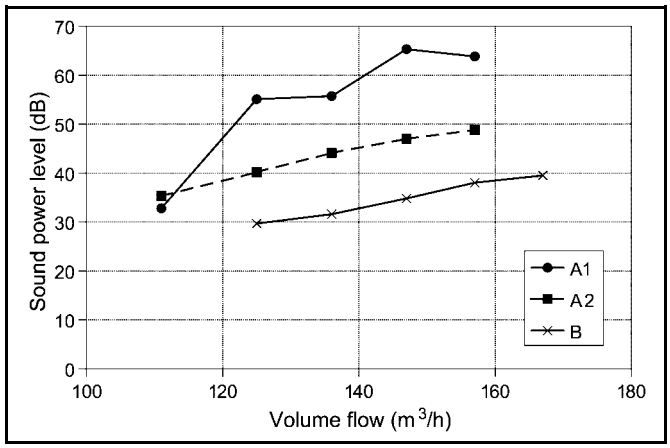

Figure 5. Total sound power level as the function of flow through the condensers.

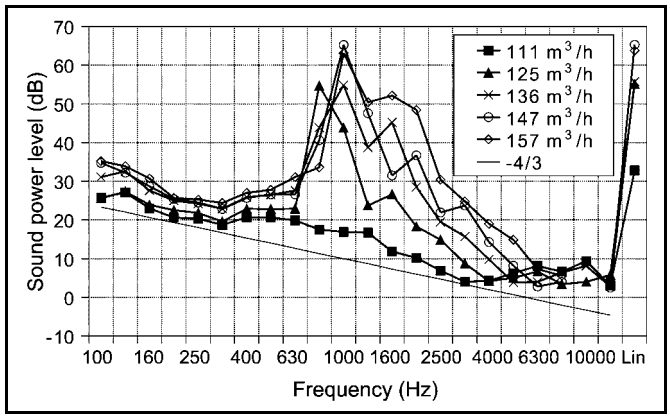

Figure 6. Sound power level spectra – condenser A1. The straight line represents the Rubinstein-Zhou scaling law $\omega^{-4/3}$ of sound power spectra radiated by isotropic turbulence. Two peaks superimposed on this non-specific background at about 1000 and 2000 Hz can be discerned, their intensity varying with the volume flow through the condenser, as indicated on the figure.

For the loudest condenser, A1, at the flow rate of 125 m^3/h, we see what can be discerned as two marked tones of sound power level at a frequency of about 1000 and 2000 Hz (Fig. 6). The intensity of the peaks depends markedly on the flow rate, as seen from the figure. The non-specific parts of the sound power level frequency spectra are consistent with algebraic frequency scaling of the form $\omega^{-4/3}$, derived from the sweeping hypothesis of time correlations by Rubinstein and Zhou.[7]

Similar conclusions may also be reached from the frequency characteristic of the sound pressure level (Fig. 7). The maximal detected sound pressure level was measured using microphone 6 at a frequency of 1000 Hz, amounting to 60.8 dB.

Condenser B shows lower sound power levels than condenser A1 (Fig. 8) due to a different flow channel design. The frequency spectrum shows two (or maybe one broad) tone components at 500 and 1000 Hz, nearly inaudible due to the low level. The non-specific part of the sound power frequency spectrum is again consistent with the $\omega^{-4/3}$ scaling law. A general observation in this case is that the specific

peaks superimposed on the non-specific background are much less pronounced than in the case of condenser A1.

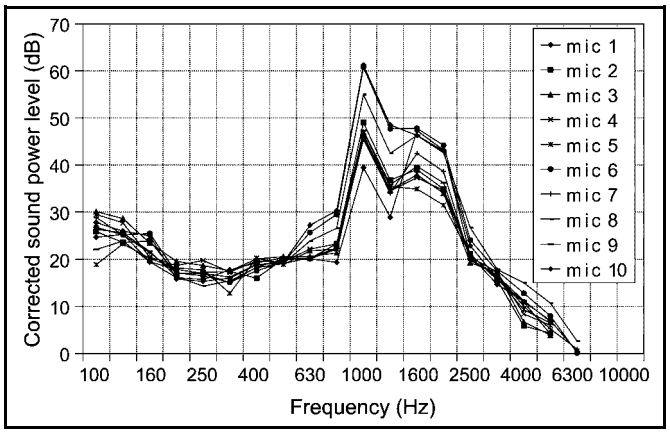

Figure 7. Corrected sound pressure level at $r = 1$ m in accordance with Table 1, condenser A1, volume flow 157 m^3/h.

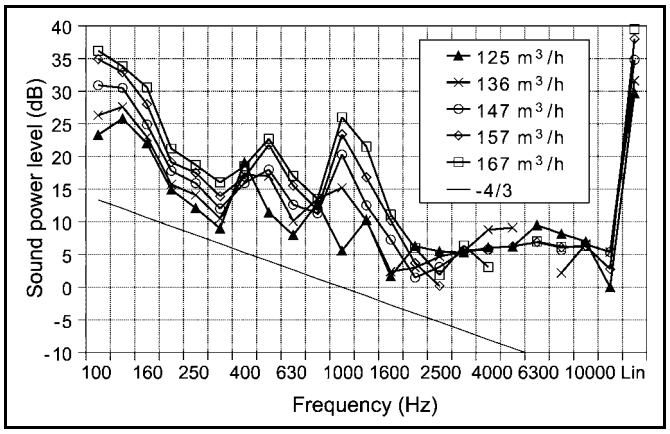

Figure 8. Sound power level spectra – condenser B. The straight line again represents the Rubinstein-Zhou scaling law $\omega^{-4/3}$ of sound power spectra radiated by isotropic turbulence. Two peaks superimposed on this non-specific background at about 500 and 1000 Hz can be discerned, their intensity again varying with the volume flow through the condenser, as indicated in the figure.

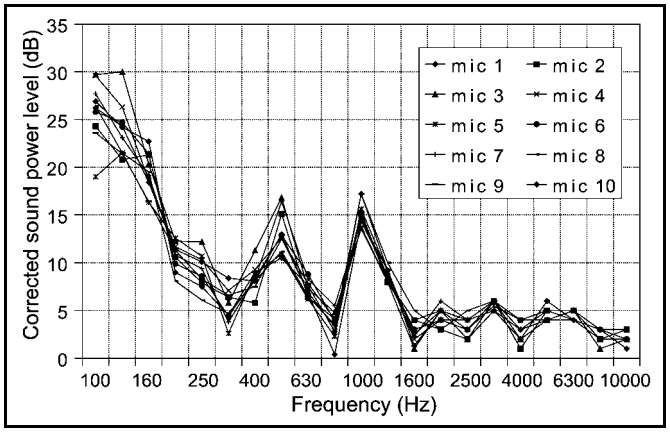

Figure 9. Corrected sound pressure level at $r = 1$ m in accordance with Table 1, condenser B, volume flow 157 m^3/h.

The frequency characteristics of the sound pressure level of condenser B are shown in Fig. 9. The maximal detected sound pressure level was measured using microphone 3 at a frequency of 125 Hz, amounting to 30 dB.

By measuring the sound intensity, we visualised the flow of sound energy in the A2 and B condensers at the flow rate of 125 m^3/h (Fig. 10). The sound power level through the frontal plane, calculated by the sound intensity method, amounts to 38.2 dB for the A2 condenser and 30.6 dB for the B condenser. If this is compared to the absolute method of determining the total sound power level, accounting for 40.2 and 29.7 dB, respectively, we may conclude that the sound intensity method gives a slightly different result. The radiation map in the B condenser demonstrates a marked density of sound energy flow, concentrated in the central part of the outlet surface, and resulting from the flow channel design.

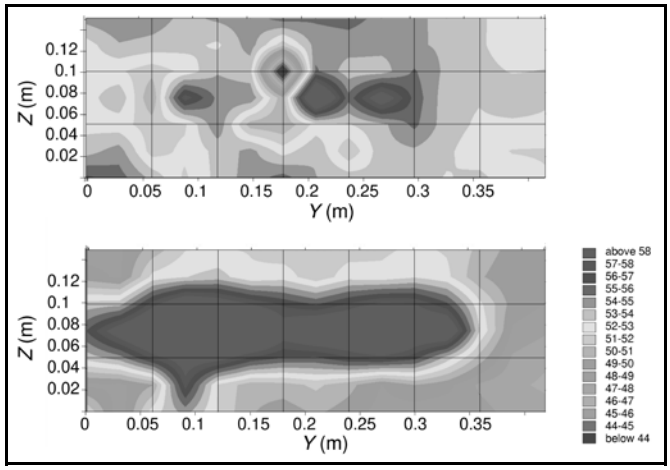

Figure 10. Sound intensity level in A2 condenser (above) and B condenser (below). The flow rate is 125 m^3/h. The scale is the same for both cases.

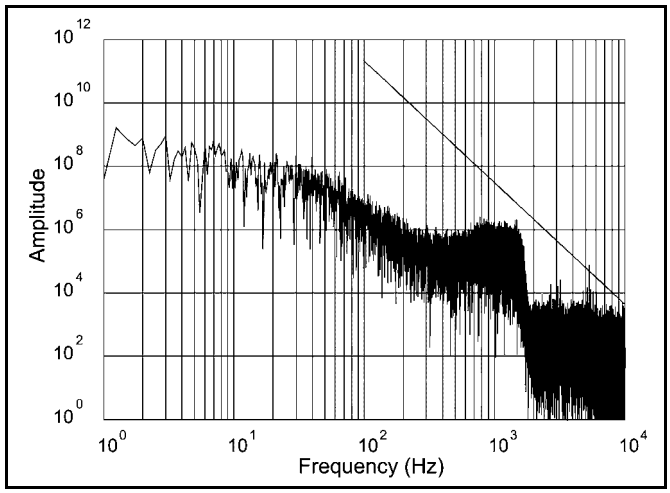

Figure 11. Power spectra of velocity fluctuations – condenser A1. The straight line represents –5/3 turbulence decay law.

Velocity power spectra are shown in Figs. 11 and 12. The velocity power spectra of condenser A shows a marked peak in fluctuations at frequencies between 1000 and 1500 Hz, and the spectra correspond to the –5/3 turbulence decay law from 100 Hz up to 10 kHz, where the filtering was applied.[4] The sound power level spectrum of condenser B does not show any peak in the frequency spectrum and can be consistently fitted to the –5/3 turbulence decay law.

The classical theories of predicting the frequency of the noise generated on a grid of rods or on a perforated sheet terminating a duct predict a discrete frequency of noise[15] radiated by periodic vortex shedding of a Karman vortex street. Turbulent flow in the condensers, however, does not show such behaviour, since the frequency peak widths were from 1

to 2 decades. The source of the noise generation by turbulent fluctuations in the condenser is quite complicated, and the noise itself is probably not generated by a regular Karman vortex street alone.

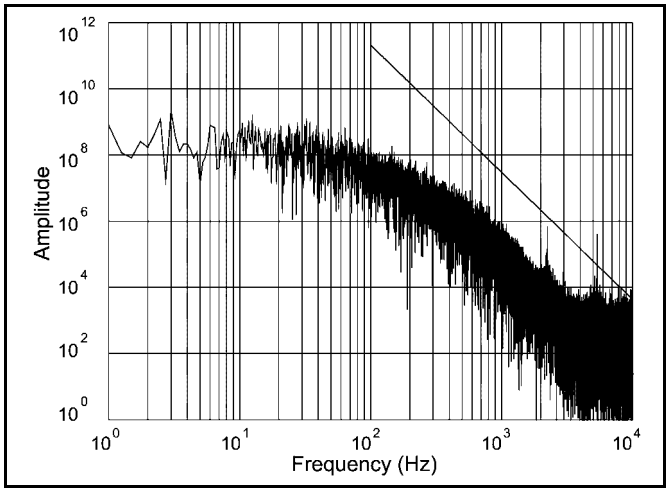

Figure 12. Power spectra of velocity fluctuations – condenser B. The straight line represents –5/3 turbulence decay law.

We have found that the power spectra of velocity fluctuations in condensers A1 and B both express similar behaviour, except in the frequency range from approximately 500 to 1500 Hz, where a peak of fluctuations is present for condenser A1. We assume that this peak of velocity fluctuations is responsible for high levels of radiated sound power level, as shown in Figs. 5 and 6. Since noise in the case of condenser A1 is presumably induced by velocity fluctuations at the outlet of the condenser, measurements of velocity fluctuations of the optional condenser under test for determination of its energetic properties can be used also as a measure of the acoustical acceptance. Establishment of energetic properties requires measurement of local velocity fluctuations, which must be approximately of the same intensity over the entire cross section of the secondary flow to enable proper condensation over the condenser's entire volume.

5. CONCLUSIONS

Development trends in large household appliances have been increasingly oriented toward noise reduction. For the case of a clothes dryer machine, we estimated the interdependence between the noise sources of the secondary circuit at the outlet side of the condenser and the aerodynamic characteristics of condenser.

Measurements of total sound power level and sound power level frequency spectrum for two types of condensers have shown marked differences. The two condensers investigated in this report differ by up to 25 dB and generally this difference increases with volume flow rate. The maximum sound power of condenser A1 is emitted in the frequency interval from 1000 to 2500 Hz, and corresponds to two specific peaks in the sound power frequency spectrum that are superimposed on the non-specific background associated with the Lighthill mechanism for isotropic turbulence at the outlet of the condenser. In condenser B we observe a similar situation, except that in this case the position and intensity of the specific peaks is different.

In order to improve the design of condensers, given that their energetic characteristics are acceptable, we propose a design that would tend to eliminate the specific peaks in the far-field noise spectra where a large proportion of the sound energy is stored. In this respect, the condenser of the type B, with its less pronounced specific peaks, definitely fares much better than condenser A. As a further direction of work, we propose a much more detailed determination of velocity dynamics at any given spatial scale in connection with the frequency distribution of the sound energy of condensers of more varied types.[16]

Under test conditions,[10] the clothes dryer with condenser A1 installed has a 5 dB higher A-weighted sound power level than with condenser B installed. This is already a noticeable difference from the operator's viewpoint, although the installation location of the home appliances has considerable influence on the overall sound power level. The other valuable consequence for the producer of the appliance is the increase in sales potential for this home appliance.

Acknowledgements

This work was partially supported by the Ministry of Education, Science and Sport, Slovenia (Contract No. L2-6591-0782-04/2.05) and Program EUREKA (Contract CONDENDRYER-E2848). This support is gratefully acknowledged.

REFERENCES

[1] Širok, B., Novak, M., Holeček N., and Lah, J. Reduction of the sound power level through a partial optimization of the aerodynamic characteristics of the flow tract of a clothes dryer, 51st International Appliance Technical Conference, Lexington, Kentucky, 2000, Proceedings of Conference, 503-513, (2000).

[2] Howe, M.S. *Theory of vortex sound*, Cambridge University Press, Cambridge, (2002).

[3] Goldstein, M.E. *Aeroacoustics*, McGraw-Hill, New York, (1976).

[4] Hinze, J.O. *Turbulence*, 2nd ed., McGraw-Hill, New York, (1975).

[5] Proudman, I. The Generation of Noise by Isotropic Turbulence, Proceedings of the Royal Society of London. Series A, *Mathematical and Physical Sciences*, **214 A** (1116), 119-132, (1952).

[6] Rubinstein, R., and Zhou, Y. The Frequency Spectrum of Sound Radiated by Isotropic Turbulence, *Physics Letters A*, **267** (5-6), 379-383, (2000).

[7] Zhou, Y., and Rubinstein, R. ICASE Report, 95-77, Sweeping and straining effects in sound generation by high Reynolds Number Isotropic Turbulence, (1995).

[8] Lilley, G.M. The Radiated Noise from Isotropic Turbulence with Applications to the Theory of Jet Noise, *Journal of Sound and Vibration*, **190** (3), 463-476, (1996).

[9] Crocker, M.J. Recent advances in acoustics and vibration, Invited Keynote Papers, Proc. First Congress of Slovenian Acoustical Society, Portoroz, Slovenia, 47-66, (1998).

[10] Lilley, G. M., Zhang, X., and Rona, A. The progress in computational aero acoustics in predicting the noise radiated from turbulent flow, *International Journal of Acoustics and Vibration*, **2** (1), 3-10, (1997).

[11] DIN 1952, Flow measurements with panels, nozzles and Venturi tubes in full flow pipes with circular cross-section, Deutsches Institut for Normung e.v., Berlin, (1982).

[12] ISO 3745, Determination of sound power levels of noise sources - Precision methods for anechoic and semi-anechoic rooms, International organization for standardization, (1977).

[13] Holeček, N., Acoustical Laboratory in Gorenje, Invited Papers, Proc. First Congress of Slovenian Acoustical Society, Portoroz, Slovenia, 369-374, (1998).

[14] Crocker, M.J. Sound Intensity, Chapter 14 in *Handbook of Acoustical measurements and Noise Control*, Harris C.M. (Ed.), Third Edition, New York, (1991).

[15] Beranek, L.L. *Noise and Vibration Control*, Institute of the Noise Control Engineering, Revised Edition, Cambridge, (1988).

[16] Rubinstein, R., and Zhou, Y. ICASE Report, 97-7, Time Correlations and the Frequency Spectrum of Sound Radiated by Turbulent Flows, (1997).